

Hydrosilated Dendritic Networks of POSS Cores and Diacetylene Linkers

Manoj K. Kolel-Veetil,^{*,†} Dawn D. Dominguez,[†] Christopher A. Klug,[‡] and Teddy M. Keller[†]

[†]Advanced Materials Section, and [‡]Materials Magnetic Resonance Section, Chemistry Division, Naval Research Laboratory, Washington, D.C. 20375.

Received October 24, 2008; Revised Manuscript Received April 15, 2009

ABSTRACT: Inorganic–organic hybrid dendritic networks containing POSS cores were constructed using two different vinyl-terminated diacetylene linker ligands via hydrosilylation reactions. FT-IR and DSC evaluations of the thermal polymerization of the diacetylene ligands indicated that such polymerizations occurred via a diradical mechanism in both long-range ordered and short-range ordered regimes at ~ 110 °C and ~ 310 °C, respectively, within the networks. The networks were further characterized by solid-state ^{13}C and ^{29}Si CPMAS NMR measurements. The hydrosilated networks possess exceptional thermal and thermo-oxidative stabilities, with the degradation temperature of one being 485 °C in N_2 and 400 °C in air. The glass transition temperatures of the networks were found to be between 40 and 60 °C by rheological measurements. Rheological properties of the networks were examined as a function of the degree of diacetylene polymerization.

Introduction

The recent surge of interest in materials derived from polyhedral oligomeric silsesquioxanes (POSS) clusters stems from the exceptional material properties of these nanoscale versions of silica. POSS clusters are known to enhance the use temperature, oxidation resistance, surface hardening and mechanical properties of polymers upon incorporation.¹ POSS clusters are also incorporated into polymers to enhance their luminescent properties.² The expectations of such property enhancements are further heightened when POSS clusters are incorporated as core entities in inorganic–organic hybrid dendritic edifices, as such architectures have well-defined internal connectivity which give them access to unique properties and functions that are sometimes unavailable to their linear counterparts. The linker groups that enable the construction of such dendritic systems can further embellish the properties of the constructed systems if they possess unique abilities such as responsiveness to external stimuli.³ In this regard, diacetylene ligands merit particular interest since their polymerization derivatives, polydiacetylenes (PDAs),⁴ exhibit strong optical absorption and fluorescence emission that change dramatically with various stimuli, such as optical exposure (photochromism),⁵ heat (thermochromism),⁶ applied stress (mechanochromism),⁷ changes in chemical environment,⁸ and binding of specific chemical or biological targets to functionalized PDA side-chains (affinochromism/biochromism).⁹

Inorganic–organic hybrid polymers containing POSS clusters also have the potential to function as space-survivable materials when used as coatings owing to their superior surface adhesion on substrates and the ability to protect bulk material from vacuum ultraviolet radiation degradation and atomic oxygen collisions.¹⁰ Furthermore, a diacetylene-linked POSS system should be able to absorb the vacuum ultraviolet radiation through its diacetylene groups resulting in the cross-linking of such groups and in the reinforcement of the coating.⁴ Most importantly, improvements in the thermal stability of such POSS-containing polymers can arise from the barrier effect to oxygen¹¹ and the limited molecular mobility of the network segments imparted by POSS–POSS interactions.¹²

Networks of POSS with rigid diacetylene linkers can also be targeted for forming materials of controlled porosity.¹³ The cubic POSS octamers offer cage structures with high surface area similar to those found in zeolites.¹⁴ The removal of the templated organic group such as diacetylene by calcination, chemical oxidation, chemical rearrangements or hydrolysis can further augment the porosity with additional pores whose size and shape will roughly correspond to that of the eliminated moiety.

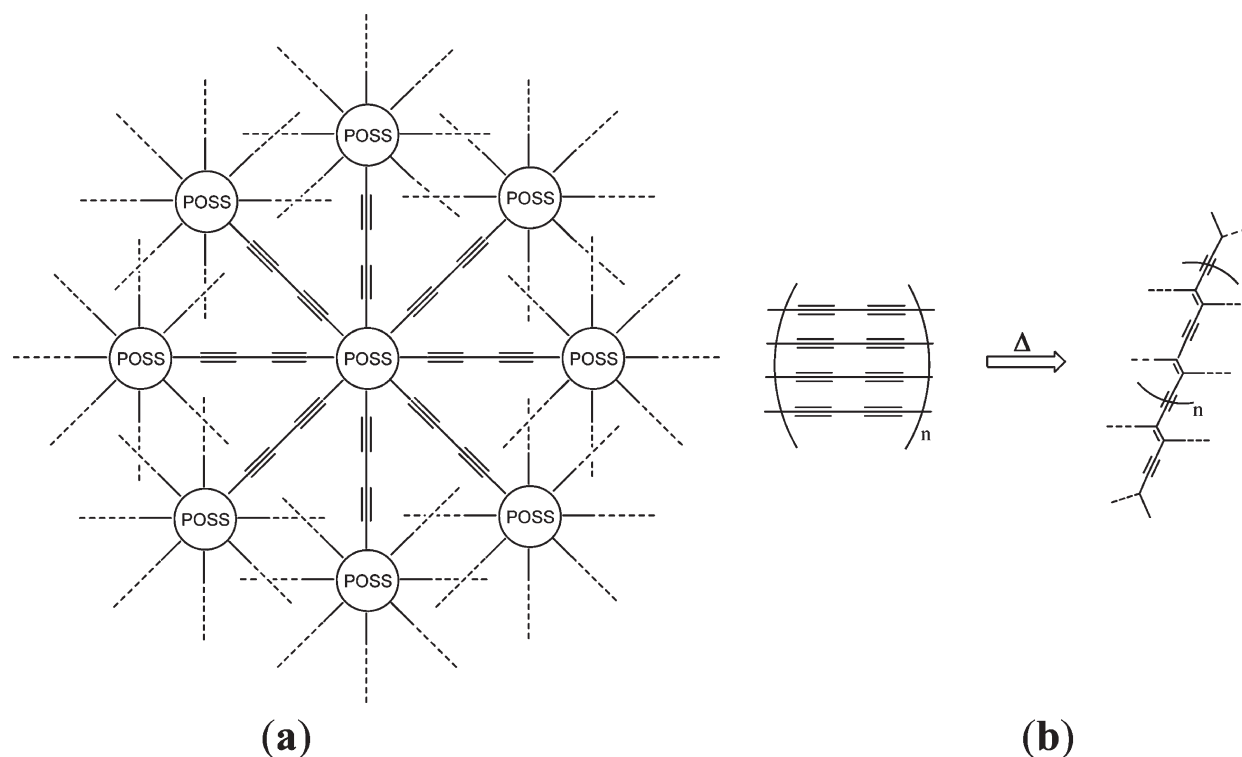
Hydrosilylation, the addition of a Si–H bond across an unsaturated organic moiety, is a ubiquitous reaction available for the construction of the alluded inorganic–organic hybrid dendritic diacetylene-linked POSS networks. It has been used to create dendritic edifices of POSS materials, including one containing both POSS and carborane clusters within its network.¹⁵ In this paper, we utilize the hydrosilylation reaction for interlinking monomeric POSS clusters **1** (Figure 1) with diacetylene-containing vinyl-terminated silane linkers **2a** or **2b** (Figure 1) to produce novel inorganic–organic hybrid dendritic networks with enhanced thermal and thermo-oxidative stabilities, that have potential for responsiveness to external stimuli, and for utility in the generation of space-survivable materials and porous materials. The thermal and thermo-oxidative stabilities of the hydrosilated networks, with POSS units possessing 3-dimensional interconnectivity via diacetylene ligands, were further improved by the mechanical reinforcement of the networks by the polymerization of the diacetylene ligands (Scheme 1). The synthesis and material properties of the developed networks are described below.

Experimental Section

Materials and Instrumentation. The POSS monomer OctaSilanePOSS (**1**) and the Karstedt catalyst (platinum–divinyl tetramethyldisiloxane complex in xylene, 2.1–2.4% Pt) were procured from Hybrid Plastics, Inc. and Gelest, Inc., respectively, and were used as received. Vinyltrimethylchlorosilane and vinylbiphenylchlorosilane, purchased from Gelest, Inc., were distilled under argon at their boiling points, 82 and 125 °C, respectively, prior to use. Toluene (anhydrous, 99.8%), *n*-butyllithium (*n*-BuLi, 2.5 M solution in hexanes), tetrahydrofuran (THF, anhydrous, 99.9%), diethyl ether (Et_2O , anhydrous, 99.5%), chloroform-*d*

*Corresponding author. E-mail: Manoj.kolel-veetil@nrl.navy.mil.

Scheme 1. Schematic Representations of (a) the Proposed Inorganic–Organic Hybrid Dendritic Networks **3a**(Hydrosilated) (R = Methyl) and **3b** (Hydrosilated) (R = Phenyl), and (b) the 1,4-Addition of the Diacetylene Ligands, an Available Pathway, during the Thermal Polymerization **3a** (Hydrosilated) or **3b**(Hydrosilated) into **3a**(Polymerized) or **3b**(Polymerized), Respectively, of This Study^a



^aThe “R” groups have been omitted for clarity and should have appeared on the diacetylene-containing linkers.

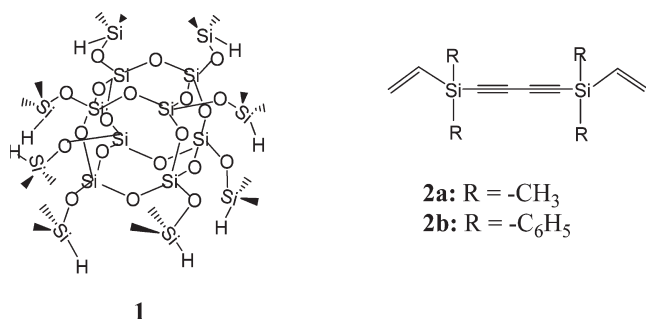
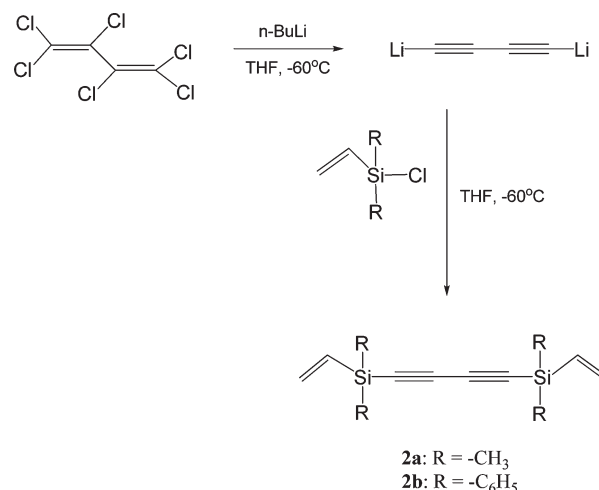


Figure 1. The POSS monomer octasilane-POSS **1**, the core entity, and the diacetylene-containing vinyl-terminated silane linkers, **2a** and **2b**, of this study.

(CDCl₃, 99.6 + atom %D), ammonium chloride (NH₄Cl, 99.5 + %), granular sodium sulfate (Na₂SO₄, anhydrous, 99 + %), activated carbon (Darco 4–12 mesh, granular), and filter agent, Celite 521 (Celite), were all obtained from Aldrich and used as received. Hexachloro-1,3-butadiene (C₄Cl₆, 97%, Aldrich) was vacuum-distilled (220 mT, 49.5 °C). **Caution!** C₄Cl₆ is toxic as are most other chlorinated reagents. The syntheses were performed under an atmosphere of dry argon utilizing standard Schlenk techniques. The preparation of 1,4-dilithio-1,3-butadiyne (dilithiodiacetylene), a precursor of **2a** and **2b**, was an adaptation of a literature procedure.¹⁶ Note: Due to the exothermic nature of the reaction during the dilithiodiacetylene production, a strict adherence to the reaction conditions is highly recommended. It has been the experience, however, of the authors that the diacetylene unit is rather inert once incorporated into the network, undergoing cross-linking only upon heating above 100–200 °C for several hours. The diacetylene-containing

Scheme 2. Reaction Scheme for the Synthesis of the Diacetylene-Containing Vinyl-Terminated Silane Linkers **2a** or **2b** via Dilithiodiacetylene



vinyl-terminated silane linkers **2a** and **2b** were synthesized as depicted in Scheme 2.

Thermogravimetric analyses (TGA) were performed on a SDT 2960 simultaneous DTA-TGA analyzer. The differential scanning calorimetry (DSC) studies were performed on a DSC 2920 modulated DSC instrument from –60 to 400 °C. All thermal experiments (TGA and DSC) were carried out at heating rates of 10 °C/min and nitrogen or air flow rate of 100 cm³/min. Infrared (IR) spectra were obtained as films on NaCl plates for the starting materials and as free-standing thin films of the various produced dendritic networks using a

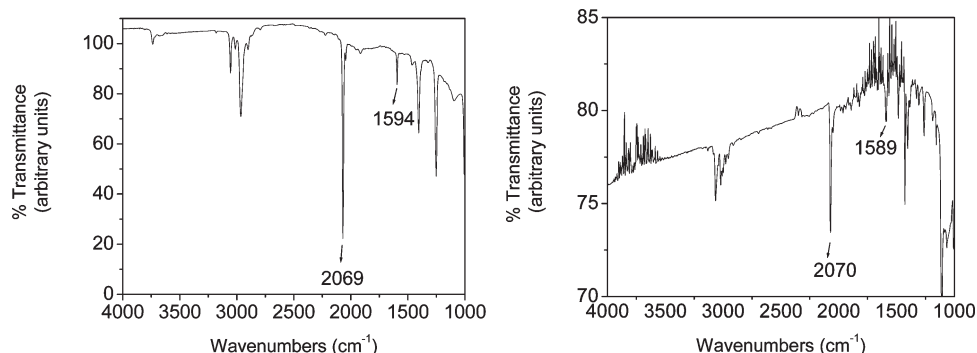


Figure 2. FT-IR spectrum of **2a** (left) and of **2b** (right) depicting the diacetylene and vinyl absorptions.

Nicolet Magna 750 Fourier transform infrared spectrometer. Solution-state ^1H and ^{13}C NMR spectra were acquired on the starting materials using a Bruker AC-300 spectrometer and referenced to the peak of the internal solvent, CDCl_3 . The solid-state NMR experiments were carried out on **3a**(hydrosilated) and **3a**(polymerized) using a Bruker DMX500 (11.7 T) spectrometer operating at Larmor frequencies of 125.8 and 99.3 MHz for ^{13}C and ^{29}Si , respectively. A triple-tuned magic-angle spinning (MAS) probe was used. The 4 mm zirconia rotors containing roughly 80 mg of sample were spun at 12.5 kHz with automatic spinning control. Recycle delays of up to 64 s were used in direct polarization experiments while a recycle delay of 4 s was used in ^1H - ^{13}C and ^1H - ^{29}Si cross-polarization (CP) experiments. The ^{29}Si , ^{13}C , and ^1H $\pi/2$ pulse lengths were 5 μs and TPPM decoupling of ^1H was used during detection. Tetramethylsilane was used as an external chemical shift reference for both ^{13}C and ^{29}Si . Rheological measurements were performed from ambient temperature to 400 $^\circ\text{C}$ in a nitrogen atmosphere on a TA Instruments AR-2000 rheometer in conjunction with an environmental testing chamber for temperature control. Measurements on rectangular solid samples were carried out in the torsion mode at a maximum strain of 2.4×10^{-4} and a frequency of 1 Hz. The samples were prepared in silicone molds with cavity dimensions of 52 mm \times 12 mm \times 2 mm by transferring flowable reaction mixtures into the molds followed by gelation and concurrent expulsion of solvent at room temperature. The storage modulus (G') and loss tangent ($\tan \delta$) were determined as a function of temperature in the 25–400 $^\circ\text{C}$ temperature range at a heating rate of 3 $^\circ\text{C}/\text{min}$.

Synthesis of 2a or 2b. Anhydrous THF (50 mL) and *n*-BuLi (46.7 mL, 2.5 M, 116.75 mmol) were transferred to a sealed 50-mL Kjeldahl reaction flask containing a magnetic stir bar. The reaction flask had been evacuated under vacuum and backfilled with argon prior to the additions. The flask was then immersed in a dry ice/2-propanol bath. While stirring, C_4Cl_6 (5 mL, 32 mmol) was added dropwise over 20 min, forming a blue, then purple, and then black solution. The dry ice/2-propanol bath was removed and the reaction mixture was warmed to room temperature with stirring over 2 h. The mixture was then recooled in a dry ice/2-propanol bath and vinyltrimethylchlorosilane (8.3 mL, 60 mmol) or vinylphenylchlorosilane (13.5 mL, 60 mmol) was added dropwise to initiate the formation of **2a** or **2b**, respectively. The reaction mixture was further warmed to room temperature with stirring over 2 h and the contents were then poured into a saturated NH_4Cl solution (150 mL, aqueous) at 0 $^\circ\text{C}$. The reaction flask was then rinsed with Et_2O into the NH_4Cl quench solution. The resulting two-phase mixture was transferred to a 500-mL separatory funnel and washed with a saturated $\text{NH}_4\text{Cl}(\text{aq})$ solution until the pH was neutral and,

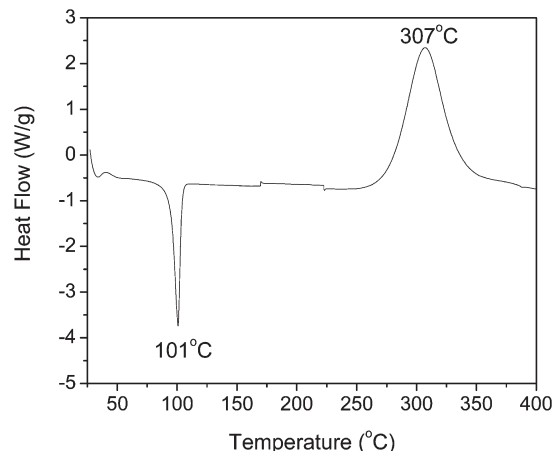


Figure 3. DSC thermogram of the crystalline **2b**, depicting the melting endotherm and the exotherm during the polymerization of the diacetylene moieties.

subsequently, twice with distilled H_2O . The dark organic phase was poured into an Erlenmeyer flask and dried over anhydrous Na_2SO_4 and activated carbon. The dried solution was filtered through Celite into a round-bottomed flask, concentrated by rotary evaporation, and then exposed to reduced pressure at room temperature for 5 h. In the case of **2a**, a brownish-red solution was obtained. Distillation of this brownish-red solution yielded **2a** as a clear reagent. In the case of **2b**, a brownish-red solid was collected. Crystallization of the solid from its concentrated solution in Et_2O yielded pale red crystals of the (divinyldiphenylsilyl)- μ -diacetylide reagent.

FT-IR. **2a**: $\nu(-\text{C}\equiv\text{C}-\text{C}\equiv\text{C}-)$: 2069 cm^{-1} and $\nu(-\text{CH}=\text{CH}_2)$: 1594 cm^{-1} (Figure 2). **2b**: $\nu(-\text{C}\equiv\text{C}-\text{C}\equiv\text{C}-)$: 2070 cm^{-1} and $\nu(-\text{CH}=\text{CH}_2)$: 1589 cm^{-1} (Figure 2). ^1H NMR (in ppm): **2a**: 6.18–5.83 ($-\text{CH}=\text{CH}_2$) and 0.26 ($-\text{CH}_3$). **2b**: 7.68–7.38 (C_6H_5-) and 6.51–5.99 ($-\text{CH}=\text{CH}_2$). ^{13}C NMR (in ppm): **2a**: (135.76, 134.62) ($-\text{CH}=\text{CH}_2$) (sp^2 C), (89.62, 84.79) ($-\text{C}\equiv\text{C}-\text{C}\equiv\text{C}-$) (sp C) and -1.27 ($-\text{CH}_3$) (sp^3 C). **2b**: (132.25, 131.87) ($-\text{CH}=\text{CH}_2$) (sp^2 C), (91.89, 81.90) ($-\text{C}\equiv\text{C}-\text{C}\equiv\text{C}-$) (sp C) and (138.04, 135.41, 130.45, 128.11) (C_6H_5-) (sp^2 C). DSC analysis in N_2 of **2b**: Melting endotherm at 101 $^\circ\text{C}$ and exotherm at 307 $^\circ\text{C}$ (Figure 3).

Formation of the Inorganic–Organic Hybrid Hydrosilated Dendritic Network, 3a(Hydrosilated), from Reaction of 1 and 2a. Octasilane–POSS **1** (0.5 g, 0.49 mmol) and **2a** (0.43 g, 1.96 mmol), at a Si–H:vinyl ratio of 1:1, were mixed with 2.5 mL of toluene to yield a clear solution. To this solution, 45 μL (4.95 μmol of Pt) of the Karstedt catalyst solution was added and the mixture was mixed vigorously for 2 min using a mechanical stirrer. The solution took on a pale yellow hue

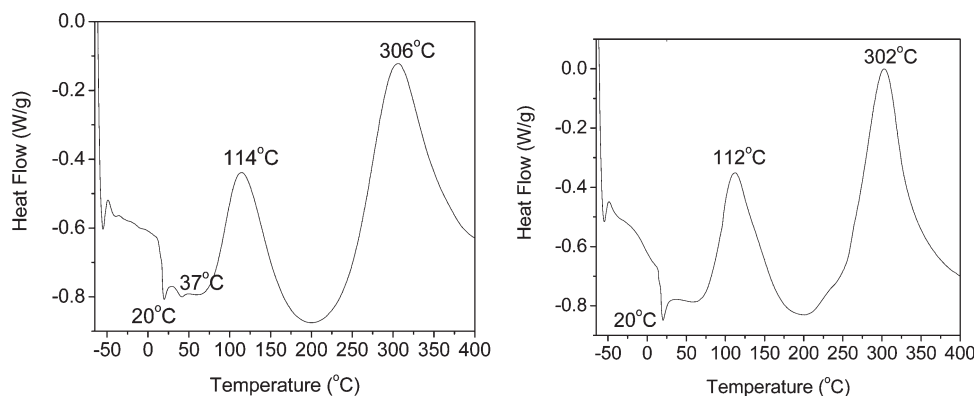


Figure 4. DSC thermograms of **3a**(hydrosilated) (left) and **3b**(hydrosilated) (right) in N_2 .

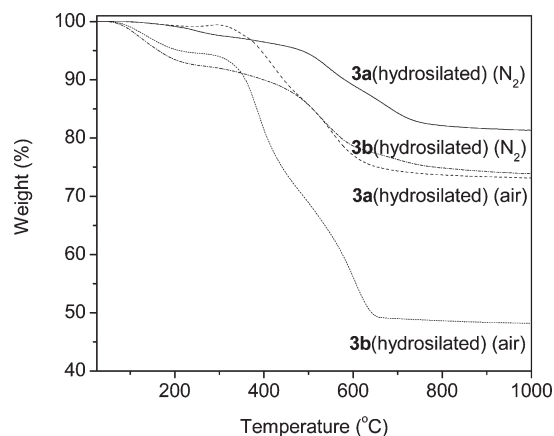


Figure 5. TGA thermograms of **3a**(hydrosilated) and **3b**(hydrosilated) in N_2 and in air.

indicating the initiation of the hydrosilylation reaction. The mixture was then transferred into a Teflon mold to facilitate the formation of a clear and transparent film at ambient conditions. DSC analysis of a film sample of **3a**(hydrosilated) under a flow of N_2 : An endotherm at 20 °C and exotherms at 114 and 306 °C were observed in the thermogram (Figure 4). TGA analysis of a film sample of **3a**(hydrosilated): In N_2 , a 5% weight loss was observed at 485 °C and the weight retention at 1000 °C was 81%. In air, a 5% weight loss occurred at 400 °C and the weight retention at 1000 °C was 73% (Figure 5).

Thermal Polymerization of the Diacetylene Units in 3a (Hydrosilated) To Form 3a(Polymerized). A well-formed, free-standing film of **3a**(hydrosilated) was thermally ramped under argon in an oven to 400 °C in an hour and was heated at this temperature for 2 h. Subsequently, the film was cooled to room temperature in 1 h. This resulted in the formation of a dark red **3a**(polymerized) film. TGA analysis of a film sample of **3a**(polymerized): In N_2 , a 5% weight loss occurred at 587 °C and the weight retention at 1000 °C was 88%. In air, a 5% weight loss occurred at 448 °C and the weight retention at 1000 °C was 79%.

Formation of the Inorganic–Organic Hybrid Hydrosilated Dendritic Network 3b(Hydrosilated) from Reaction of 1 and 2b. Octasilane–POSS **1** (0.50 g, 0.49 mmol) and **2b** (0.91 g, 1.96 mmol), at a Si–H:vinyl ratio of 1:1, were mixed with 2.5 mL of toluene to yield a clear solution. To this solution, 90 μ L (9.90 μ mol of Pt) of the Karstedt catalyst solution was added and the mixture was mixed vigorously for 5 min using a mechanical stirrer. The solution remained clear indicating that the initiation of the hydrosilylation reaction had not occurred. Hence, the mixture was transferred into a Teflon

mold and was heated on a hot plate at 80 °C for 1 h to facilitate the formation of a clear and transparent film. DSC analysis of a film sample of **3b**(hydrosilated) in N_2 : An endotherm at 20 °C and exotherms at 112 and 302 °C were observed in the thermogram (Figure 4). TGA analysis of a film sample of **3b**(hydrosilated): In N_2 , a 5% weight loss occurred at 164 °C and the weight retention at 1000 °C was 74%. In air, a 5% weight loss occurred at 218 °C and the weight retention at 1000 °C was 49% (Figure 5).

Thermal Polymerization of the Diacetylene Units in 3b (Hydrosilated) To Form 3b(Polymerized). A well-formed, free-standing film of **3b**(hydrosilated) was thermally ramped under argon in an oven to 310 °C in an hour and was heated at this temperature for 2 h. Subsequently, the film was cooled to room temperature in 1 h. This resulted in the formation of a dark red **3b**(polymerized) film.

Results and Discussion

Dilithiodiacetylene¹⁶ is a versatile reagent that can be utilized in producing the proposed dendritic inorganic–organic hybrid system with POSS cores, as it can function as a rigid linking group or upon functionalization at its termini. The functionalization of the dilithiodiacetylene at its termini can be affected by various halogenated ligands possessing reactive end groups by the delithiation reaction that produces the corresponding lithium halide. In the present study, the lithiated termini of the dilithiodiacetylene were reacted with vinyltrimethylchlorosilane or vinyl-diphenylchlorosilane to produce corresponding vinyl-terminated diacetylene-containing cross-linkers **2a** and **2b** (Scheme 2). Furthermore, the proposed dendritic networks of **1**, shown in Scheme 1, require that the linker ligands **2a** or **2b** be functionalized at their termini rather than at the internal alkyne moieties of its diacetylene group during the synthesis. In this regard, it was anticipated that the terminal alkene groups in **2a** or **2b** would preferentially function as sites for hydrosilylation reactions over the internal diacetylene groups, with the eight available symmetrically disposed reactive Si–H bonds of the octasilane–POSS cluster, **1**. This assumption was based on the expectation that the reactive Si–H groups tethered to the bulky octasilane–POSS ligand, **1**, would exhibit diminished reactivity to the internal diacetylene due to steric encumbrance. With regard to observed selectivities in hydrosilylation reactions, it is relevant to note here that a typical R_3SiH ligand is known to add to terminal olefins at a higher rate than to internal olefins.¹⁷ However, an R_3SiH ligand has also been shown to add at a greater rate to an internal alkyne than to a terminal olefin in Karstedt catalyst-catalyzed hydrosilylation reactions.¹⁸ No example exists of a system where such comparisons are made on a single compound containing both a terminal alkene and an internal alkyne or an internal diacetylene (1,3-diyne). The diacetylene ligand is known to be susceptible to

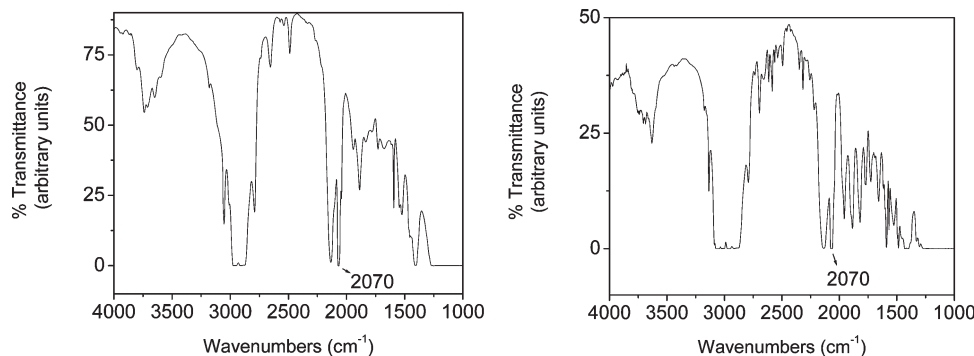


Figure 6. FT-IR spectrum of **3a**(hydrosilylated) (left) and of **3b**(hydrosilylated) (right) depicting the diacetylene absorption contained in the networks.

both single and double hydrosilylations depending on the hydrosilylation catalyst and the reaction conditions.¹⁹ Interestingly, with the Karstedt catalyst, it has been reported that even a single addition of the R_3SiH resulted in poor yield ($\sim 36\%$) of the product even at $80^\circ C$ after 1 day, when one of the R groups in the R_3SiH reactant was a bulky ligand such as $OSiMe_3$.²⁰ Thus, with an R_3SiH ligand such as **1** where one of the R groups is $-O-(RSiO_{1.5})_8$, which is much bulkier than $OSiMe_3$, it can be expected that the addition of the $Si-H$ bonds under ambient temperature will occur preferentially at the terminal alkene instead of the internal diacetylene of **2a** and **2b** during the hydrosilylation reactions. In fact, during a unimolar hydrosilylation reaction of **2a** with a bulky silane such as *t*-butyldimethylsilane or triphenylsilane, (results to be published), the $Si-H$ bond was observed to add, by both Markonikov and anti-Markonikov modes,²¹ at one of the terminal alkene groups rather than at the internal diacetylene group of **2a**. Hence, it follows that the formation of the postulated dendritic structure of the inorganic-organic hybrid network (Scheme 1) seems reasonable upon reaction of **1** with **2a** or **2b**.

The physical states of the two linker ligands **2a** and **2b** were found to be different at ambient conditions. While **2a** was found to be a clear liquid, **2b** was obtained as a crystalline solid. However, the spectroscopic characteristics of **2a** and **2b** were found to be very similar. The internal diacetylene and the terminal vinyl vibrational absorptions were observed at 2069 and 1594 cm^{-1} for **2a**, and at 2070 and 1589 cm^{-1} for **2b**, respectively, in their FT-IR spectra (Figure 2). The ^{13}C resonances of the sp^2 carbons of the terminal vinyl groups were present at 135.76 and 134.62 ppm for **2a** and at 132.25 and 131.87 ppm for **2b** as observed from their solution ^{13}C NMR spectra. Similarly, the ^{13}C resonances of the sp carbons of the diacetylene group were observed at 89.62 and 84.79 ppm for **2a** and 91.89 and 81.90 ppm for **2b**, respectively. The similarity in the IR frequencies and ^{13}C resonances of the vinyl and diacetylene groups in **2a** and **2b** suggested that the electronic environments of these groups in **2a** and **2b** were almost identical. This apparent equivalence in their electronic states, however, did not produce comparable hydrosilylation reaction rates with **1** owing to the differences in the steric demands at the reactive vinyl groups in **2a** and **2b** (*vide infra*).

The crystalline linker **2b** was further investigated to ascertain whether its diacetylene groups could be polymerized by thermal means in its solid-state. During solid-state polymerization of diacetylenes, elongated polymer chains can be formed under preservation of the starting crystalline phase structure provided that the molecular motions accompanying chemical transformation compensate each other in a way to minimize the overall changes of the crystallographic parameters.²² The DSC thermogram of the crystalline **2b**, exhibited a melting endotherm at $101^\circ C$ and a broad exotherm at $307^\circ C$ (Figure 3). Therefore, it appears that in **2b**, the thermal polymerization of the diacetylene

triple bonds occurs in a disordered amorphous phase and not in a solid-state/crystalline state.²³

During the formation of the dendritic networks from **1** and **2a** or **2b**, the onset and progress of the reaction were monitored by the FT-IR characterization of the reaction mixture. A gradual disappearance of the vinyl absorption of **2a** or **2b** at 1594 and 1589 cm^{-1} , respectively, and the disappearance of the $Si-H$ absorption at 2140 cm^{-1} of the octasilane-POSS **1** (Figure 6) indicated the progress of the reaction. The addition of $Si-H$ bonds of **1** to the alkene groups of **2a** and **2b** is believed to proceed by both Markonikov and anti-Markonikov modes, as observed in the reaction of **2a** with *tert*-butyldimethylsilane or triphenylsilane. After the initial hydrosilylation reactions, the diacetylene absorptions in both **3a**(hydrosilylated) and **3b**(hydrosilylated) networks appeared at 2070 cm^{-1} . However, some unreacted vinyl groups of **2a** and **2b** and unreacted $Si-H$ bonds of **1** were also observed in the FT-IR spectrum of the reaction products. Thus, it appears that all of the 8 reactive $Si-H$ bonds in a POSS cluster may not be accessible for reaction at ambient temperature with the terminal vinyl groups in **2a** and **2b** due to steric crowding around the POSS cluster. This situation in the generated networks is not surprising considering the fact that the linker groups **2a** and **2b** are not particularly long. Soxhlet extractions of the products were performed in toluene to determine whether there was any unreacted **2a** or **2b** entrapped in the networks. The small amount of *sol* fraction (less than 2%) suggested that almost the entire amount of the linkers were bound, at least at one of their termini, to the POSS clusters in the generated networks. The progress of the reaction can also be monitored by 1H , ^{13}C and ^{29}Si NMR spectroscopy.

The reaction of **1** with **2a** was found to proceed easily at room temperature in comparison to its reaction with **2b**, which was found to be sluggish at ambient temperature. In order to obtain a similar extent of reaction of **1** with **2b** as with **2a**, the mixture of **1** and **2b** had to be treated with twice the amount of the Karstedt catalyst and had to be heated at $80^\circ C$ for 1 h. The diminished reactivity of the alkene groups of **2b** in comparison to the vinyl groups of **2a** is presumed to be due to the steric encumbrance caused by the two bulkier phenyl groups on the Si atom containing the alkene group in **2b** in comparison to the two sterically less demanding methyl groups on the Si atom that contains the alkene group in **2a**. Similar effects of steric factors on the rates of addition of $Si-H$ across double bonds are known and the additions have been reported to occur more facily at the least hindered side or face (when the hydrosilylated ligand is of a cyclic type).^{20,24}

Solid-state ^{13}C CPMAS NMR spectrum of the **3a**(hydrosilylated) network exhibited multiplets in the 80–110 ppm range for the sp^2 C resonances of the diacetylene group in the **2a** linker with partially and completely reacted alkene groups (Figure 7). The resonances were observed as broad signals at 108, 104, 90, and 85 ppm. These include a doublet set of resonances for the

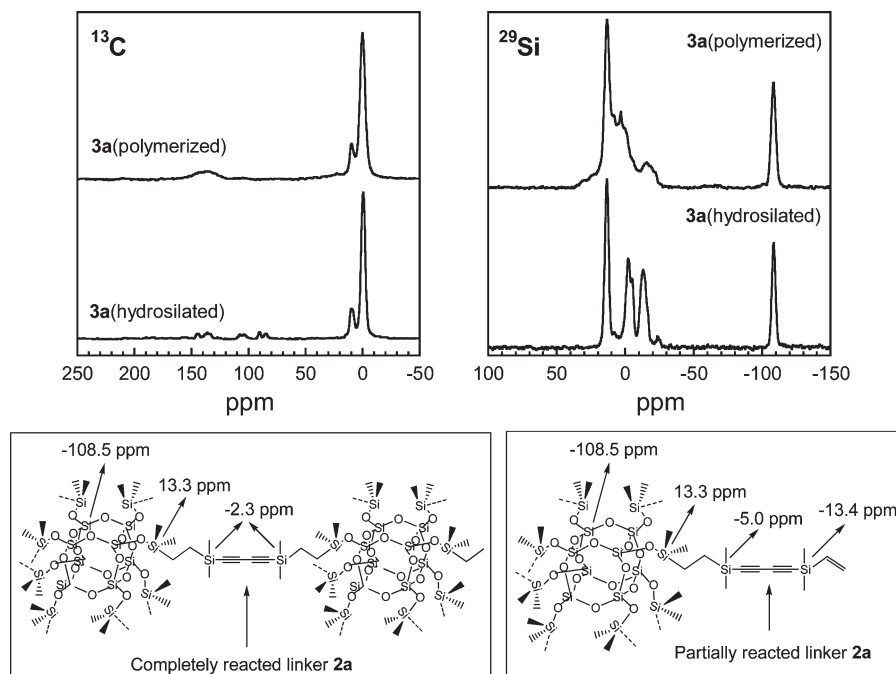


Figure 7. Top panels: ^{13}C and ^{29}Si CPMAS spectra of **3a**(hydrosilated) and **3a**(polymerized). Bottom panels: Various representative ^{29}Si chemical shifts in **3a**(hydrosilated) containing partially and completely reacted **2a** linkers.

diacetylene group of the completely reacted **2a** linker and two quartet sets of resonances for the diacetylene groups arising from the Markonikov and anti-Markonikov additions of Si–H to one of the alkene groups of the partially reacted **2a** linker, as seen for the products of the unimolar hydrosilylation reactions of **2a** and bulky silane *t*-butyldimethylsilane or triphenylsilane. The corresponding sp^2 C resonances for the unreacted alkene group of the partially reacted **2a** linker were observed between 130 and 150 ppm. In addition, the sp^3 C resonances of the reacted alkene group of **2a** were observed at 10 ppm and the sp^3 C resonances of the Si-bound methyl groups of both **1** and **2a** were observed at 0 ppm. In the solid-state ^{29}Si CPMAS NMR spectrum of the **3a** (hydrosilated) network, the cluster Q4 silicon atoms²⁵ of **1** appeared at -108.5 ppm and the peripheral M-type Si atoms were seen at 13.3 ppm (Figure 7). In comparison, the corresponding resonances of **1** are -109.2 ppm and -2.3 ppm, respectively. Thus, the resonances of the cluster Si atoms remained virtually unchanged whereas the resonance of the M-type Si atoms, which is carbon-bound in **3a**(hydrosilated), shifted upfield by more than 15 ppm. The ^{29}Si resonances related to the reacted **2a** linker were observed at -2.3 , -5.0 , and -13.4 ppm. The appearance of these three new resonances, in place of the single ^{29}Si resonance of -23.4 ppm for the neat **2a** linker, supports the existence of partially and completely reacted **2a** in the network. The resonances of the silicon atoms in the completely reacted **2a** is assigned to -2.3 ppm and the resonance of the silicon atom attached to the alkene that is consumed in the partially reacted **2a** appears at -5.0 ppm and the remaining silicon attached to the unreacted alkene appears at -13.4 ppm. All of these resonances appear shifted upfield when compared to the single resonance of the neat **2a** linker. The various types of Si atoms in **3a**(hydrosilated) with their corresponding ^{29}Si NMR chemical shifts are depicted schematically in Figure 7.

The hydrosilated network **3a**(hydrosilated), with intact internal diacetylene groups, was observed to be extremely thermally stable as evidenced by its high temperature of degradation (temperature of 5% weight loss) of 485°C and its high weight retention of 81% at 1000°C when heated in a N_2 atmosphere (Figure 5). The 19% weight loss at 1000°C corresponded to a loss of about three-quarters of the labile Si-bound methyl groups in

the network, since Si, O, and the carbons of the diacetylene groups are not known to be lost at such conditions unless present in pendant groups.^{23,26} In this regard, of the total 32 methyl groups in a repeat dendritic unit in **3a**(hydrosilated), half of the Si-bound methyl groups belong to the peripheral Si atoms of the dimethylsiloxyl groups of **1** and the other half are bound to the Si atoms of the **2a** linker. The $\sim 19\%$ weight loss corresponds to a loss of 24 Si-bound methyl groups. Of particular interest, then, is the question as to which of the Si-methyl groups get retained upon cross-linking and formation of **3a**(hydrosilated). An answer to this becomes apparent when the TGA thermogram of **3b** (hydrosilated) network is analyzed (Figure 5). In **3b**(hydrosilated), there are 16 Si-bound methyl groups on the peripheral Si atoms of the dimethylsiloxyl groups of **1** and 16 Si-bound phenyl groups on the Si atoms of **2b** linker. The weight loss of $\sim 26\%$ at 1000°C in this network requires that at least 8 phenyl groups of the linker ligand be retained in the final product, since a loss of all the phenyl groups of **2b** would have brought the final char yield to around 55%. By extrapolation, it appears that the retention of 8 methyl groups and 8 phenyl groups on thermal treatment of **3a** (hydrosilated) and **3b**(hydrosilated) to 1000°C in N_2 , respectively, occur at the Si atoms of the linkers **2a** and **2b**. Similarly, the weight loss, at 1000°C in air, of 27% for **3a**(hydrosilated) and of 51% for **3b**(hydrosilated) represent a complete loss of all the pendant methyl and phenyl groups in the two systems. This suggests that the treatment of **3a**(hydrosilated) and **3b**(hydrosilated) to 1000°C in air should yield dendritic systems containing only cross-linked diacetylene groups as the organic functionality. The removal of the diacetylene groups in such thermo-oxidatively treated networks by calcination, chemical oxidation or hydrolysis can be expected to yield highly porous materials similar to zeolites with high surface area.^{13,14} The exceptional thermal and thermo-oxidative stabilities of **3a**(hydrosilated) and **3b**(hydrosilated) networks can be attributed to the barrier effect to oxygen exhibited typically by POSS-containing systems¹¹ and to the suppression of the molecular mobility of polymer segments¹² by the bulky POSS and the rigid diacetylene groups in the network. Similar suppression of molecular mobility in POSS-containing inorganic–organic hybrid networks has been suggested to be the reason for their high thermal stability as it reduces

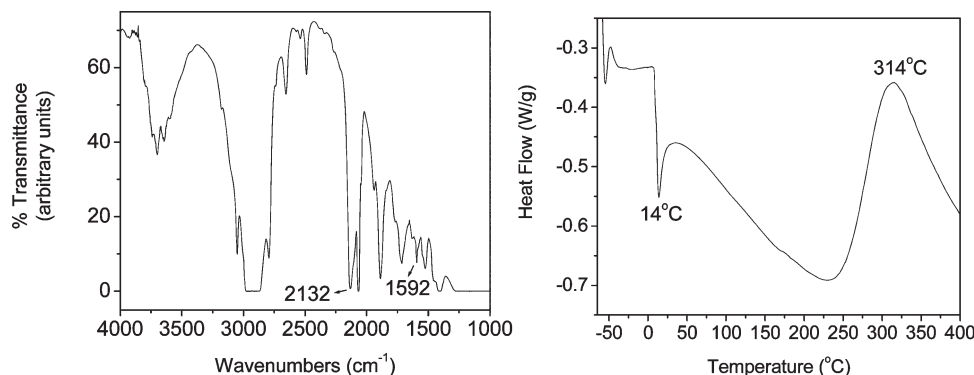


Figure 8. FT-IR spectrum (left) and DSC thermogram (right) of a **3a**(hydrosilated) film after thermal treatment at 150 °C for 4 h.

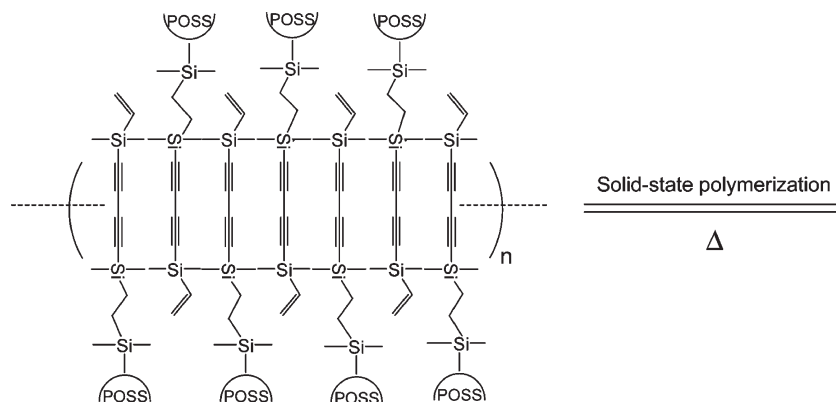


Figure 9. 2-Dimensional depiction of the interdigitation of partially reacted **2a** linkers bound to clusters of **1** involved in the solid-state polymerization at ~110 °C in **3a**(hydrosilated).

transport of reactive species within the polymer due to an enhancement in the activation energy^{11a} and, furthermore, due to the retardation of the release of volatiles at higher temperatures.^{11b}

In investigating the thermal polymerization of diacetylenes in **3a**(hydrosilated) and **3b**(hydrosilated), it was of utmost interest to determine whether the polymerization occurred in a solid-state or rather in a disordered amorphous phase, as observed in **2b**. The DSC thermogram of **3a**(hydrosilated) (Figure 4) exhibited an endotherm at 20 °C and exotherms at 114 and 306 °C. However, an important aspect to consider was whether the two exotherms were a result of distinct events of diacetylene polymerizations in **3a**(hydrosilated). Since the exotherm at 306 °C was presumed to have originated from the thermal polymerization of diacetylenes, for example, as observed similarly in **2b**, it was necessary to determine the origin of the 114 °C exotherm. Hence, a film of **3a** (hydrosilated) was treated at 150 °C for 4 h in N₂ to ensure the completion of the exothermic event around 114 °C. During this thermal treatment, the sample took on a red hue suggestive of the thermal polymerization of diacetylenes. The FT-IR spectrum and the DSC thermogram of the treated sample were obtained to further examine the origin of the exothermic event (Figure 8). The FT-IR spectrum exhibited the retention of the vibrations of unreacted Si–H bonds of **1** and the vinyl groups of **2a**. This suggested that the exotherm at 114 °C originated from the thermal polymerization of diacetylenes and not from another exothermic event such as the reaction of any residual Si–H bonds of **1** and the vinyl groups of **2a**. In addition, the DSC thermogram of the treated sample to 400 °C in N₂ exhibited only a single exotherm at 315 °C, indicating the complete disappearance of the diacetylene units in **3a**(hydrosilated) that caused polymerization attributed to the exotherm at 114 °C. Thus, it appears that the lower exotherm at 114 °C represents a solid-state type

polymerization of diacetylenes and the higher exotherm at 306 °C belongs to a polymerization of diacetylenes in an amorphous disordered state in **3a**(hydrosilated). The solid-state type regions in **3a**(hydrosilated) probably originated from the interdigitation of diacetylene units belonging to proximal partially reacted (bound at a single terminus) **2a** linkers attached to clusters of **1** as shown in Figure 9. The low temperature (114 °C) of the initial exotherm for this solid-state polymerization of the diacetylenes in an ordered crystalline-like phase in comparison to the higher temperature (306 °C) for the diacetylene polymerization in the disordered amorphous regions is not surprising considering reports that solid-state polymerization of diacetylenes can occur even at room temperature and very easily at 80 °C.²⁷ A similar DSC thermogram (Figure 4) was also observed for **3b**(hydrosilated) with an endotherm at 20 °C and exotherms at 112 and 302 °C, which suggested that the dendritic systems in the two cases were very similar.

The operation of two distinct events of thermal polymerization of diacetylene units during the thermal treatment of **3a**(hydrosilated) is apparent in the FT-IR spectrum of the resulting polymerized product **3a**(polymerized) (Figure 10), which was obtained upon the complete thermal polymerization of the diacetylene units in **3a**(hydrosilated) heated to 400 °C. The absorptions at 2132 and 1890 cm^{−1} in the FT-IR spectrum can be attributed to ene-yne²⁸ and butatriene²⁹ functionalities, respectively, that are produced upon thermal polymerization of the diacetylene units of **3a**(hydrosilated) to varying degrees of repeat units. It is known that the dicarbene or the diradical moieties (Figure 11) function as chain initiators for the formation of an ene-yne or a butatriene-type of polymerization, respectively. In the case of the diradical intermediate, its energy of formation is lower than that of the dicarbene moiety, since its formation requires the disruption of only one C–C π -bond instead of two in

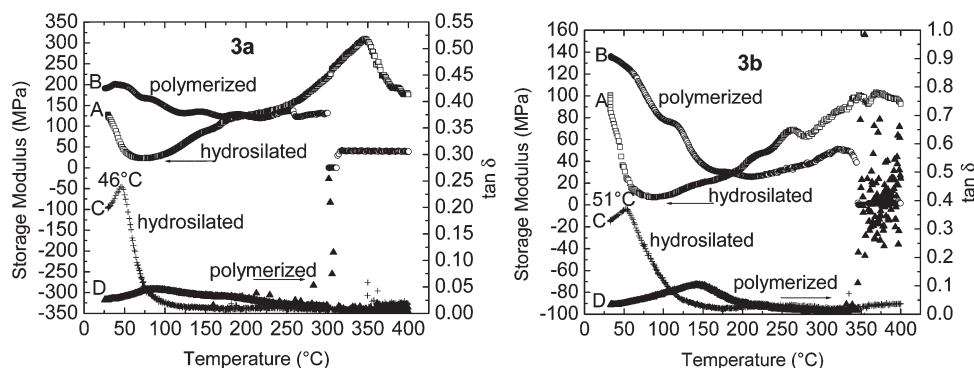


Figure 12. Storage modulus (G') and loss tangent ($\tan \delta$) of the various dendritic networks of this study. Left: **3a**(hydrosilated) and **3a**(polymerized). Right: **3b**(hydrosilated) and **3b**(polymerized). Plots A and B: G' . Plots C and D: $\tan \delta$.

rendered nondeformable under high-strain conditions thereby nullifying an improvement in the domains' cohesion by the development of stronger nonbonded forces. Such domain cohesion was achieved only under an optimum level of diacetylene polymerization.³³ Hence, it is presumed that above 330 °C, further polymerization probably reduced G' of **3a**(hydrosilated) due to the formation of possible nondeformable domains in the network. To verify this, a sample of **3a**(hydrosilated) was initially thermally treated to 400 °C in N_2 to produce **3a**(polymerized) and subsequently its G' was evaluated. The G' value at ambient temperature was found to be equal to ~ 190 MPa as obtained for **3a**(hydrosilated) at 400 °C during its rheological run. The thermal treatment of **3b**(hydrosilated) to 400 °C in N_2 for 2 h, on the other hand, was found to produce an extensively brittle sample, which was found not usable for rheological evaluations, indicating that upon diacetylene polymerization an even greater degree of nondeformable domains were formed in such a sample than in **3a**(polymerized). Hence, a sample of **3b**(hydrosilated) was treated to 310 °C for 1 h to produce an intact sample of **3b**(polymerized) and a rheological measurement was performed on this sample. As anticipated, the G' (~ 140 MPa) of this sample at ambient temperature was found to be higher than that of the ambient temperature G' (~ 100 MPa) of the 'as prepared' **3b**(hydrosilated).

Conclusions

The inorganic–organic hybrid dendritic networks containing POSS cores developed in this study appear to have potential for use as porous materials, space-survivable materials and as materials that are responsive to external stimuli. Toward realizing such potential, the impressive thermal and thermo-oxidative stabilities of these networks should aid in their utilization under extremely demanding conditions. Furthermore, the utilization of these networks as stimuli-responsive materials will be facilitated if the diacetylene polymerization in the networks can be controllably varied especially to desired long-range orders ($n > 6$ repeat units) as required for such applications. For example, an enhancement in the degree of solid-state polymerization may be attained by augmenting the crystallinity in these networks. To achieve such an enhancement, incorporation of linkers of increasing chain lengths between the POSS clusters of **1** can, perhaps, lead to beneficial segments in the networks that can pack into solid-state domains favorable for long-range ordered polymerization of diacetylenes at lower temperatures. In fact, recent studies of polydiacetylene/silica nanocomposites comprising long linking diacetylene units with attending alkyl units such as $(CH_2)_8$, $(CH_2)_9$, $(CH_2)_{11}$, etc. on either termini have reported the polymerization of the diacetylene units in the 90–110 °C temperature range.³⁴ The composites were also observed to exhibit thermochromatic properties.

Acknowledgment. The authors thank the Office of Naval Research for its financial support of this work.

References and Notes

- (1) (a) Pittman, C. Jr.; Li, G.-Z.; Ni, H. *Macromol. Symp.* **2003**, *196*, 301–325. (b) Li, G.-Z.; Wang, L.; Ni, H.; Pittman, C. Jr. *J. Inorg. Organomet. Polym.* **2001**, *11* (3), 123–154.
- (2) Chen, K.-B.; Chang, Y.-P.; Yang, S.-H.; Hsu, C.-S. *Thin Solid Films* **2006**, *514* (1–2), 103–109.
- (3) Carpick, R. W.; Sasaki, D. Y.; Marcus, M. S.; Eriksson, M. A.; Burns, A. R. *J. Phys.: Condens. Matter* **2004**, *16*, R679–R697.
- (4) Bloor, D.; Chance, R. R., Eds.; *Polydiacetylenes: Synthesis, Structure, and Electronic Properties*; Martinus Nijhoff and Springer Verlag LLC: Dordrecht, The Netherlands, and New York, 1985.
- (5) (a) Day, D.; Hub, H. H.; Ringsdorf, H. *Isr. J. Chem.* **1979**, *18*, 325–334. (b) Tieke, B.; Lieser, G.; Wegner, G. *J. Polym. Sci., Part A* **1979**, *17*, 1631–1644. (c) Olmsted, J.; Strand, M. *J. Phys. Chem.* **1983**, *87*, 4790–4792. (d) Carpick, R. W.; Sasaki, D. Y.; Burns, A. R. *Langmuir* **2000**, *16*, 1270–1278.
- (6) (a) Wenzel, M.; Atkinson, G. H. *J. Am. Chem. Soc.* **1989**, *111*, 6123–6127. (b) Lio, A.; Reichert, A.; Ahn, D. J.; Nagy, J. O.; Salmeron, M.; Charych, D. H. *Langmuir* **1997**, *13*, 6524–6532. (c) Chance, R. R.; Baughman, R. H.; Muller, H.; Eckhardt, C. J. *J. Chem. Phys.* **1977**, *67*, 3616–3618. (d) Carpick, R. W.; Mayer, T. M.; Sasaki, D. Y.; Burns, A. R. *Langmuir* **2000**, *16*, 4639–4647. (e) Lee, D. C.; Sahoo, S. K.; Cholli, A. L.; Sandman, D. J. *Macromolecules* **2002**, *35*, 4347–4355.
- (7) (a) Muller, H.; Eckhardt, C. J. *Mol. Cryst. Liq. Cryst.* **1978**, *45*, 313–334. (b) Nallicheri, R. A.; Rubner, M. F. *Macromolecules* **1991**, *24*, 517–525. (c) Tomioka, Y.; Tanaka, N.; Imazeki, S. *J. Chem. Phys.* **1989**, *91*, 5694–5700. (d) Cheng, Q.; Stevens, R. C. *Langmuir* **1998**, *14*, 1974–1976.
- (8) (a) Jonas, U.; Shah, K.; Norvez, S.; Charych, D. H. *J. Am. Chem. Soc.* **1999**, *121*, 4580–4588. (b) Carpick, R. W.; Sasaki, D. Y.; Burns, A. R. *Tribol. Lett.* **1999**, *7*, 79–86.
- (9) (a) Charych, D. H.; Nagy, J. O.; Spevak, W.; Bednarski, M. D. *Science* **1993**, *261*, 585–588. (b) Reichert, A.; Nagy, J. O.; Spevak, W.; Charych, D. *J. Am. Chem. Soc.* **1995**, *117*, 829–830. (c) Charych, D.; Quan, C.; Reichert, A.; Kuziemiwo, G.; Strohm, M.; Nagy, J. O.; Spevak, W.; Stevens, B. *Chem. Biol.* **1996**, *3*, 1131–20.
- (10) Phillips, S. H.; Haddad, T. S.; Tomczak, S. J. *Curr. Opin. Solid State Mater. Sci.* **2004**, *8*, 21–29.
- (11) (a) Tejerina, B.; Gordon, M. S. *J. Phys. Chem. B* **2002**, *106*, 11764–11770. (b) Ascuncion, M. Z.; Laine, R. M. *Macromolecules* **2007**, *40*, 555–562.
- (12) (a) Janowski, B.; Pielichowski, K. *Thermochim. Acta* **2008**, *478* (1–2), 51–53. (b) Liu, H.; Zheng, S. *Macromol. Rapid Commun.* **2005**, *26*, 196–200.
- (13) Pielichowski, K.; Njuguna, J.; Janowski, B.; Pielichowski, J. *Adv. Polym. Sci.* **2006**, *201*, 225–296.
- (14) Breck, D. W. *Zeolite Molecular Sieves*; Wiley-Interscience: New York, 1984.
- (15) (a) Bassindale, A. R.; Gentle, T. E. *J. Mater. Chem.* **1993**, *3*, 1319–1326. (b) Jaffres, P.-A.; Morris, R. E. *J. Chem. Soc., Dalton, Trans.* **1998**, 2767–2770. (c) Casado, C. M.; Cuadrado, I.; Morán, M.; Alonso, B.; Barranco, M.; Losada, J. *Appl. Organomet. Chem.*

- 1999, 13, 245–259. (d) Zhang, C. X.; Laine, R. M. *J. Am. Chem. Soc.* **2000**, 122, 6979–6988. (e) Saez, I. M.; Goodby, J. W.; Richardson, R. M. *Chem.—Eur. J.* **2001**, 7 (13), 2758–2764. (f) Manson, B. W.; Morrison, J. J.; Coupar, P. I.; Jaffrès, P.-A.; Morris, R. E. *J. Mol. Catal. A: Chem.* **2002**, 182–183, 99–105. (g) Wada, K.; Watanabe, N.; Yamada, K.; Kondo, T.; Mitsudo, T.-a. *Chem. Comm.* **2005**, 95–97. (h) Chen, K.-B.; Chang, Y.-P.; Yang, S.-H.; Hsu, C.-S. *Thin Solid Films* **2006**, 514 (1–2), 103–109. (i) Seino, M.; Hayakawa, T.; Ishida, Y.; Kakimoto, M. *Macromolecules* **2006**, 39, 8892–8894. (j) Kolel-Veetil, M. K.; Dominguez, D. D.; Keller, T. M. *J. Polym. Chem.: Part A. Polym. Chem.* **2008**, 46 (7), 2581–2587.
- (16) Ijadi-Maghsood, S.; Barton, T. J. *Macromolecules* **1990**, 23, 4485–4486.
- (17) (a) Lukevics, E.; Belyakova, Z. V.; Pomerantseva, M. G.; Voronkov, M. G. In *Journal of Organometallic Chemistry Library*; Seyferth, D., Ed.; Elsevier: Amsterdam, 1977; Vol. 5, pp 1–35. (b) Eaborn, C.; Bott, R. W. The Bond to Carbon. In *Organometallic Compounds of The Group IV Elements*; MacDiarmid, A., Ed.; Marcel Dekker: New York, 1968; Vol. 1, pp 105–536.
- (18) Lewis, L. N.; Sy, K. G.; Donahue, P. E. *J. Organomet. Chem.* **1992**, 427, 165–172.
- (19) (a) Kusumoto, T.; Hiyama, T. *Chem. Lett.* **1985**, 1405–1408. (b) Kusumoto, T.; Ando, K.; Hiyama, T. *Bull. Chem. Soc. Jpn.* **1992**, 65, 1280–1288. (c) Kunai, A.; Toyoda, E.; Nagamoto, I.; Horio, T.; Ishikawa, M. *Organometallics* **1996**, 15, 75–83.
- (20) Perry, R. J.; Karageorgis, M.; Hensler, J. *Macromolecules* **2007**, 40, 3929–3938.
- (21) Marciniak, B. *Silicon Chem.* **2002**, 1, 155–176.
- (22) (a) Wegner, G. *Z. Naturforsch.* **1969**, 24B, 824–842. (b) Baughman, R. H. *J. Appl. Phys.* **1972**, 43, 4362–4370.
- (23) Corriu, R.; Gerbier, Ph.; Guérin, C.; Henner, B.; Fourcade, R. *J. Organomet. Chem.* **1993**, 449, 111–118.
- (24) (a) Weng, W.-W.; Chen, R.-M.; Luh, T.-Y. *Heteroatom. Chem.* **1995**, 6 (1), 15–18. (b) Trofimov, A.; Rubina, M.; Rubin, M.; Gevorgyan, V. *J. Org. Chem.* **2007**, 72, 8910–8920.
- (25) (a) Loy, D. A.; Baugher, B. M.; Baugher, C. R.; Schneider, D. A.; Rahimian, K. *Chem. Mater.* **2000**, 12, 3624–3632. (b) Ek, S.; Iiskola, E. I.; Niinistö, L.; Vattinen, J.; Pakkanen, T. J.; Root, A. *J. Phys. Chem. B* **2004**, 108, 11454–11463.
- (26) Corriu, R. J. P.; Moreau, J. J. E.; Thepot, P.; Man, M. W. C. *Chem. Mater.* **1996**, 8, 100–106.
- (27) (a) Bloor, D.; Koski, L.; Stevens, G. C.; Preston, F. H.; Ando, D. J. *J. Mater. Sci.* **1975**, 10, 1678–1688. (b) Wegner, G. *Makromol. Chem.* **1972**, 154, 35–48.
- (28) (a) Helveger, A. J.; Baughmann, R. H. *J. Polym. Sci., Part B: Polym. Phys.* **1989**, 27, 1853–1866. (b) Brefort, J. L.; Corriu, R. J. P.; Guerin, C.; Henner, B. J. L. *J. Organomet. Chem.* **1994**, 464, 133–142.
- (29) (a) West, R.; Chwang, T. L. *J. Am. Chem. Soc.* **1973**, 95, 3324. (b) Jaffe, F. *J. Organomet. Chem.* **1970**, 23, 53–62.
- (30) Bäessler, H.; Sixl, H.; Enkelmann, V. In *Polydiacetylenes*; Cantow, H.-J., Ed.; Advances in Polymer Science 63; Springer-Verlag: Berlin and New York, 1984; pp 1–136.
- (31) Hori, Y.; Kispert, D. *J. Am. Chem. Soc.* **1979**, 101, 3173–3177.
- (32) Goross, H.; Neumann, W.; Sixl, H. *Chem. Phys. Lett.* **1983**, 95, 584–590.
- (33) Nallicheri, R. A.; Rubner, M. F. *Macromolecules* **1990**, 23, 1017–1029.
- (34) (a) Lu, Y.; Yang, Y.; Sellinger, A.; Lu, M.; Huang, J.; Fan, H.; Haddad, R.; Lopez, G.; Burns, A. R.; Sasaki, D. Y.; Shelnutt, J.; Brinker, C. J. *Nature* **2001**, 410, 913–916. (b) Peng, H.; Tang, J.; Pang, J.; Chen, D.; Yang, L.; Ashbaugh, H. S.; Brinker, C. J.; Yang, Z.; Lu, Y. *J. Am. Chem. Soc.* **2005**, 127, 12782–12783. (c) Peng, H.; Tang, J.; Yang, L.; Pang, J.; Ashbaugh, H. S.; Brinker, C. J.; Yang, Z.; Lu, Y. *J. Am. Chem. Soc.* **2006**, 128, 5304–5305.